

Precipitation and temperature trends and dryness/wetness pattern during 1971–2015 in Zhejiang Province, southeastern China

Weiping Lou¹ · Lihong Wu² · Yuding Mao² · Ke Sun¹

Received: 23 July 2015 / Accepted: 20 April 2017 / Published online: 30 May 2017
© Springer-Verlag Wien 2017

Abstract This study explores change of precipitation and temperature using the Mann–Kendall test and the spatiotemporal variation of dryness/wetness using the standardized precipitation evapotranspiration index and empirical orthogonal function (EOF) analysis on 1-month time scales in Zhejiang Province, China, over 1971–2015. The results show that monthly precipitation had significant decreasing trends during April, May, September, and October, and significant increasing trends during November and December. Monthly temperatures had significant increasing trends in each month. Increasing temperature significantly increased drought events and intensity. There were consistent spatial patterns of dryness/wetness in Zhejiang. There were dryness trends in April, May, and September, a wetness trend in August, and no dryness/wetness pattern change in other months. The second EOF modes showed that dryness/wetness patterns were anti-phase between northern and southern Zhejiang during April–October. The third EOF modes showed that patterns were anti-phase between eastern and western Zhejiang in August and September.

1 Introduction

Climate change greatly alters the precipitation and temperature patterns in many countries (Guo and Xia 2014). Changes in those patterns modify wet and dry conditions and directly affect

hydrology, agriculture, ecosystems, and water resources management (Fischer et al. 2011; Zhang et al. 2009; Rebetz et al. 2006). One of the most popular indices for studying wet and dry conditions is the standardized precipitation index (SPI) developed by McKee et al. (1993), which is based on a probabilistic precipitation approach (Livada and Assimakopoulos 2007). The SPI has been used in assessing the spatiotemporal variations of dryness/wetness in many areas, because it is simple and only considers rainfall (Huang et al. 2014a). Huang et al. (2014a, b) analyzed the variability of dry and wet periods during 1961–2010 in Hunan Province, China, and 1961–2008 in Sichuan Province. They used the SPI and principal component analysis to assess climatic conditions and covariability of the stations. Yusof et al. (2014) used the SPI to analyze trend behavior for dry and wet events to verify dryness and wetness episodes in Peninsular Malaysia.

The SPI provides good estimates of the intensity of drought/wetness episodes based on spatial and temporal dimensions. The main advantage of the SPI in comparison with other indices is that it enables both the determination of drought conditions over various time scales and monitoring of different drought types (Patel et al. 2007). However, the main criticism of the SPI is that it is based only on precipitation data. The index does not consider other variables that could influence droughts, such as temperature, evapotranspiration, wind speed, and soil water-holding capacity (Vicente-Serrano et al. 2010).

Drought depends on precipitation and temperature, and empirical studies have shown that temperature rise markedly affects drought severity (Rebetz et al. 2006). Dubrovsky et al. (2009) showed that effects on drought of the warming predicted by global climate models are not reflected clearly by the SPI. Fischer et al. (2011) used temperature and precipitation data from 192 weather stations during 1961–2007 and the SPI to analyze the variability of dry and wet periods in the

✉ Weiping Lou
xclwp@163.com

¹ Xinchang Weather Bureau, Xinchang County, Zhejiang Province 312500, China

² Zhejiang Provincial Climate Center, Hangzhou 310017, China

Zhujiang River Basin of China. Their results showed that the magnitude of the index describing dryness has increased in the that basin and that the duration of dry periods has increased, whereas that of wet periods has shortened. The SPI analysis did not reveal any significant trends and no changes in dry or wet conditions were detected, which is in line with the findings of Zhai et al. (2010) and Zhang et al. (2009).

In recognition of the effect of temperature on drought, Vicente-Serrano et al. (2010) proposed the standardized precipitation–evapotranspiration index (SPEI). The SPEI is based on precipitation and temperature data, and it has the advantage of combining multiscale characteristics with the capacity to include effects of temperature variability in drought assessment. Mathematically, the SPEI is similar to the SPI, except that it includes the effect of temperature. The SPEI is based on water balance; thus, it can be compared to the self-calibrated Palmer drought severity index and is suitable for drought evaluation within the context of global warming (Vicente-Serrano et al. 2012).

Various studies have shown that it is more advantageous to apply the SPEI than other drought indices. For example, Stagge et al. (2015) compared a suite of candidate probability distributions for use in continental-scale SPI and SPEI normalizations focused on Europe, using the $0.5^\circ \times 0.5^\circ$ gridded Watch Forcing Data set. The results showed that all candidate SPEI distributions produced better fits than candidate SPI distributions, because the climatic water balance was not bounded by zero. This removed the difficulties associated with fitting piecewise distributions around this limit. Lorenzo-Lacruz et al. (2010) used the SPEI and SPI to analyze the influence of climatic variation on the availability of water resources in the headwaters of the Tagus River Basin. They found that although precipitation played a major role in explaining temporal variability within analyzed parameters, the influence of temperature was non-negligible, and responses of river discharge and reservoir storage were slightly stronger when based on the SPEI compared with the SPI. Potop et al. (2012) found that the SPEI performed better than the SPI for agricultural drought evolution over various time scales. The SPEI has also been used to evaluate meteorological, agricultural, and hydrological drought (Gocic and Trajkovic 2014; Potop et al. 2014).

Zhejiang is one of the most economically active provinces in China. However, frequent droughts and floods within this province have hindered sustainable social, economic, and ecological development and resulted in severe environmental problems. Because of its uneven spatiotemporal distribution of precipitation, complex landform characteristics, and other factors, Zhejiang experiences some of the most serious drought/flood-related disasters in southeastern China (Shen and Hu 2005). Global warming is causing variations in temperature and precipitation in Zhejiang and affecting drought/wet episodes within this province (Qian and Lin 2004, 2005).

Thus, the study of changes in dryness/wetness patterns in the province is becoming increasingly important.

The key objectives of this study were to investigate the long-term spatiotemporal trends of precipitation and temperature during 1971–2015, and to detect the trends of drought/wetness patterns using the SPEI. The results could provide a scientific basis for the management and planning of water resources in Zhejiang Province within the context of global warming.

2 Materials and method

2.1 Study region

Zhejiang Province ($27.20\text{--}31.52^\circ\text{N}$, $118.00\text{--}123.00^\circ\text{E}$) has a land area of $10.18 \times 10^4\text{ km}^2$, 70.4% of which is hills and mountains. Economically, in 2015, it was the fourth most important province in China. Zhejiang is in southeastern China, encompassing the middle and lower reaches of the Yangtze River, with the Pacific Ocean to the east (Fig. 1). Zhejiang has a subtropical climate with a strong monsoon and distinct seasons. Average winter and summer temperatures are $3\text{--}9$ and $24\text{--}28^\circ\text{C}$, respectively, and annual average temperature is $15\text{--}18^\circ\text{C}$. Average annual precipitation is $1000\text{--}2000\text{ mm}$, and precipitation during the rainy season (April–September) accounts for 60–70% of the annual total. In Zhejiang, meteorologically related disasters such as droughts, rainstorms, floods, typhoons, and cold weather occur with high frequency and large extent.

2.2 Data

Daily temperature and precipitation datasets of 75 national meteorological stations in Zhejiang Province were provided by the Network Center of the Zhejiang Provincial Meteorological Bureau (NCZP). The NCZP checked and controlled all datasets for quality and homogeneity, using the cumulative deviation test and standard normal homogeneity test (Feng et al. 2004; Fischer et al. 2011). Only 62 stations with continuous time series (no data gaps) from 1 January 1971 to 31 December 2015 were used in the present study (Fig. 1).

2.3 Methodology

We assessed the spatiotemporal variations of dryness/wetness using the SPEI, and temporal trends and spatial distributions of dryness/wetness in Zhejiang Province during 1971–2015 were examined using the Mann–Kendall test. Detailed principles of calculating the indices and method applications are described in the following text.

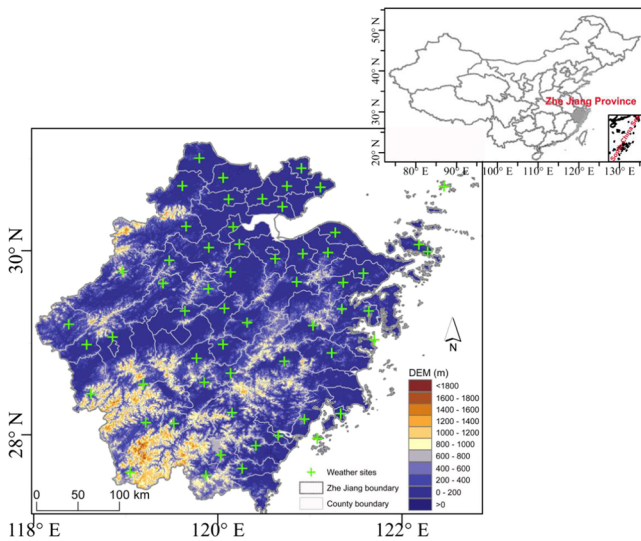


Fig. 1 The weather sites used in this study and location of Zhejiang Province, China. The DEM with a spatial resolution of 1 km is available at <http://srtm.csi.cgiar.org/>

2.3.1 Standardized precipitation–evapotranspiration index

A detailed description of the method for computing the SPEI is found in Vicente-Serrano et al. (2010). In our study, quantification of the SPEI was based on the following steps: (i) calculation of potential evapotranspiration, (ii) determination of the accumulation of deficit and/or surplus of climatological water balance over a certain time scale (difference between precipitation (RR) and evapotranspiration (ET_0)), and (iii) normalization of water balance into a generalized extreme value distribution to obtain the SPEI index series.

The United Nations Food and Agriculture Organization Penman–Monteith method was used to estimate ET_0 (Allen et al. 1998):

$$ET_0 = \frac{0.408\Delta(R_n - G) + \gamma \frac{900}{T + 273} u_2 (e_s - e_a)}{\Delta + \gamma(1 + 0.34u_2)}, \quad (1)$$

where ET_0 is the reference evapotranspiration (mm/day), R_n is the net radiation at the surface ($\text{MJ}/\text{m}^2/\text{day}$), G is the soil heat flux density ($\text{MJ}/\text{m}^2/\text{day}$), T is the mean daily air temperature (at 2 m height, $^{\circ}\text{C}$), u_2 is the wind speed (2 m height, m/s), e_s is the saturation vapor pressure (kPa), e_a is the actual vapor pressure (kPa), $e_s - e_a$ is the saturation vapor pressure deficit (kPa), Δ is the slope of the vapor pressure curve ($\text{kPa}/^{\circ}\text{C}$), and γ is the psychrometric constant ($\text{kPa}/^{\circ}\text{C}$). ET_0 was calculated at daily time step using ETo calculator version 3.2.

Water balance was calculated as the difference between precipitation (RR_i) and evapotranspiration (ET_{0i}) for month i according to

$$D_i = RR_i - ET_{0i} \quad (2)$$

which provides a simple measure of the water surplus or deficit for a month.

The calculated D_i values were then aggregated over different time scales, following the same procedure as that used for the SPI.

The generalized extreme value distribution is given for standardizing the D series to obtain the SPEI (Stagge et al. 2015). This distribution can be formulated as

$$f(x) = \begin{cases} \frac{1}{\sigma} (1 + \xi z)^{-1-1/\xi} \exp(-(1 + \xi z)^{-1/\xi}) & \xi \neq 0, 1 + \xi z > 0 \\ \frac{1}{\sigma} \exp(-z - \exp(-z)) & \xi = 0, -\infty < x < \infty \end{cases}, \quad (3)$$

where $z = \frac{x - \mu}{\sigma}$, ξ , σ , and μ are the shape, scale, and location parameters.

According to the generalized extreme value distribution, the probability distribution function of the D series can be given by

$$F(x) = \begin{cases} \exp(-(1 + \xi z)^{-1/\xi}) & \xi \neq 0, 1 + \xi z > 0 \\ \exp(-\exp(-z)) & \xi = 0, -\infty < x < \infty \end{cases}. \quad (4)$$

The SPEI is obtained as standardized values of $F(x)$:

$$\text{SPEI} = W - \frac{C_0 + C_1 W + C_2 W^2}{1 + d_1 W + d_2 W^2 + d_3 W^3}, \quad (5)$$

where

$$W = \sqrt{-2 \ln(P)} \text{ for } P \leq 0.5 \quad (6)$$

and P is the probability of exceeding a determined D value ($P = 1 - F(x)$). If $P > 0.5$, then P is replaced by $1 - P$ and the sign of the resultant SPEI is reversed. The constants are $C_0 = 2.515517$, $C_1 = 0.802853$, $C_2 = 0.010328$, $d_1 = 1.432788$, $d_2 = 0.189269$, and $d_3 = 0.001308$.

2.3.2 Trend analysis

The Mann–Kendall test can reliably identify monotonic linear and nonlinear trends in non-normal datasets with outliers. This method has been found an excellent tool for trend detection in time series data and has been used to assess the significance of trends in climatic data series (Huang et al. 2014a). In the present study, we used the Mann–Kendall test and statistical significances were inferred at $P < 0.10$, $P < 0.05$, and $P < 0.01$, respectively. Sen’s nonparametric method was used to detect the magnitude of slope changes (Sen 1968).

2.3.3 Empirical orthogonal function analysis

Empirical orthogonal function (EOF) analysis, also known as the Natural Orthogonal Component algorithm or principal component analysis, was invented by Pearson in 1901. The use of an orthogonal transformation to decompose an original dataset into a set of uncorrelated and ordered base functions, as well as associated coefficients, reduces the dimensionality of a dataset consisting of multiple intercorrelated variables, while preserving the majority of the variation caused by certain independent processes (Ercha et al. 2012). Using this method, the most efficient decomposition of the data into representative modes is done by empirically finding the eigenfunctions that best describe the information. The EOF eigenmodes can be ordered in terms of the percentage of total variance described by each mode, and the modes are statistically uncorrelated with each other. Thus, the EOF method has been used for analysis of data with complex spatiotemporal structures (Kaihatu et al. 1998). In climate studies, EOF analysis is often used to study possible spatial modes (i.e. patterns) of variability and how they change with time.

The meteorological element field is represented as follows:

$$X = (x_{ij}) = \begin{bmatrix} x_{11} & \cdots & x_{1n} \\ \vdots & \ddots & \vdots \\ x_{m1} & \cdots & x_{mn} \end{bmatrix} \quad (7)$$

where x_{ij} represented the j th value in the i th meteorological station, n is the length of meteorological element series at each meteorological station, and m is the number of meteorological stations. Through the EOF expansion, Eq. (7) is decomposed into the sum product of the orthogonal spatial matrix (V) and orthogonal time matrix (T):

$$X = VT = (x_{ij}) = \left(\sum_{k=1}^m v_{ik} t_{kj} \right) \quad (8)$$

where v_{i1}, \dots, v_{im} represent the spatial distribution of the i th EOF mode and t_{1j}, \dots, t_{mj} are the time coefficients which represent temporal variability of the j th EOF mode.

3 Results and discussion

3.1 Trends of monthly precipitation during 1971–2015

From 1971 to 2015, changes of precipitation in February–July were not significant. Precipitation in September and October decreased, and some counties had statistically significant trends ($P \leq 0.05$). Precipitation in January, August, November, and December increased, and some counties had statistically significant trends ($P \leq 0.05$) (Fig. 2).

Partial correlation coefficients of monthly precipitation and the SPEI were ≥ 0.9300 , with 0.01 significance level in all

months. Precipitation and SPEI trends were found to be identical. As monthly precipitation increased, the SPEI became larger (wetter months) and, as that precipitation decreased, the SPEI became smaller (drier months).

3.2 Trends of monthly temperature during 1971–2015

From 1971 to 2015, monthly temperatures increased in each month and some counties had statistically significant trends ($P \leq 0.05$), except for January (Fig. 3).

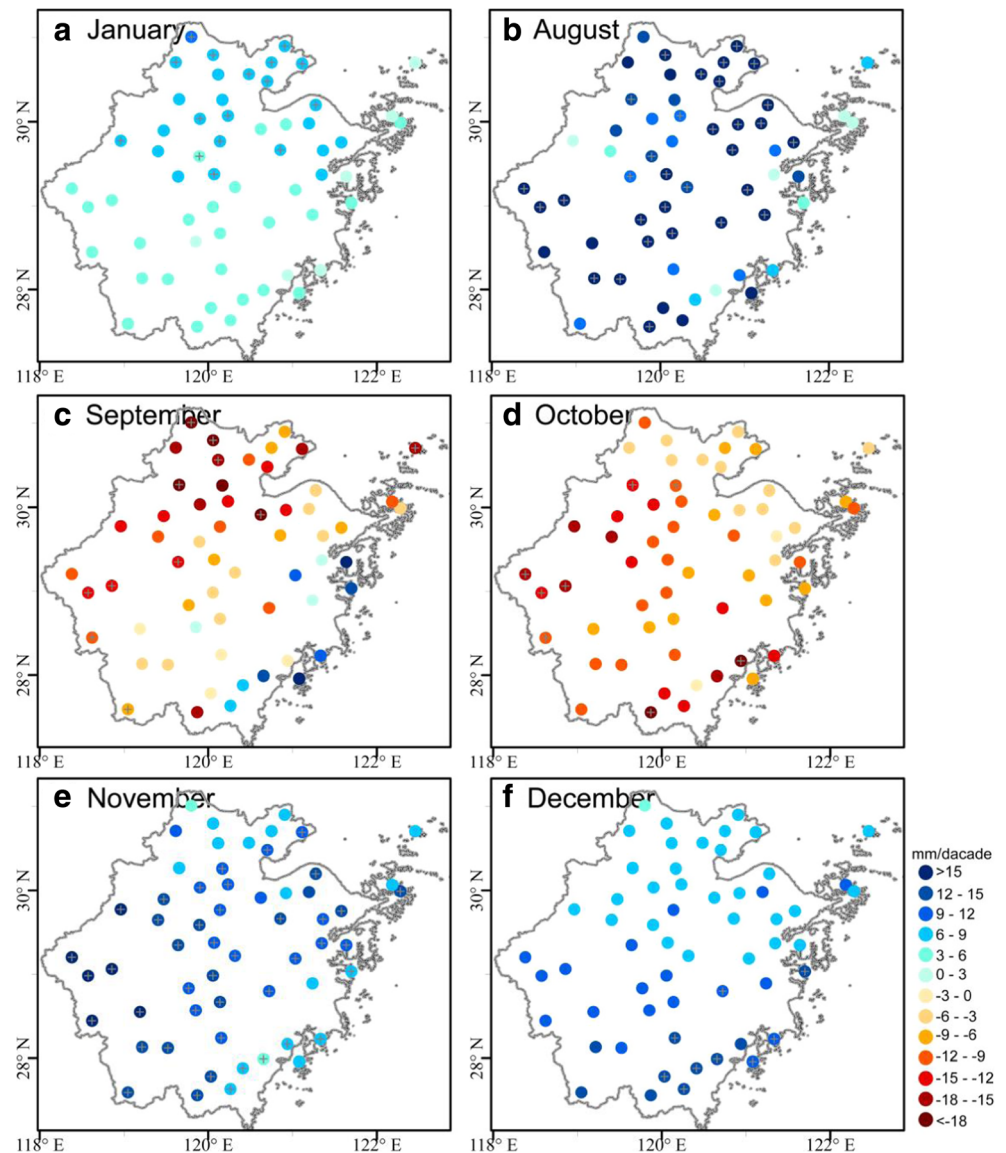
Partial correlation coefficients of monthly temperature and the SPEI were ≥ 0.3038 , with 0.05 significance level in all months. For May–September, partial correlation coefficients of monthly temperature and the SPEI were -0.6144 to -0.7399 , with 0.01 significance level. The temperature and SPEI trends were opposite. As monthly temperature increased, the SPEI declined (drier months), and as that temperature decreased, the SPEI became larger (wetter months).

3.3 Spatiotemporal variability of dryness/wetness during 1971–2015

The EOF analysis was applied to the time series of monthly SPEI for each station in Zhejiang Province. At least 70% of the variance was explained by only one mode for January–March, November, and December, by two modes for April–July and October, and by three modes for August and September (Table 1). For January–March, November, and December, differences in precipitation spatial distribution were small because of winter monsoon effects, and so differences in the dryness/wetness spatial pattern were also small. From April to the first half of July, the precipitation spatial distribution was anti-phase between southern and northern parts of Zhejiang Province, because of the interaction of cold and warm air. From the latter half of July through September, the spatial distribution was anti-phase between southeastern and northwestern parts of Zhejiang Province, because of tropical cyclones. In some years, there was more precipitation in northern Zhejiang in the latter half of August and September, because of the effect of cold air. The uneven spatial distribution of precipitation caused an uneven SPEI spatial distribution.

Spatial coefficients of the first EOF mode in all counties of Zhejiang Province were 0.01 to 0.14 in each month, indicating consistency of the dryness/wetness pattern across the province. The time coefficient of the first EOF mode showed the variation of this distribution with time. Years for which the time coefficient was >0 belonged to the wet type, e.g., May 1973 was a typical wet year in the province. Conversely, years for which the time coefficient was <0 belonged to the dry type, e.g., May 2007 was a typical dry year (Fig. 4). The time coefficients for each month exhibited no statistically significant trends, except for April, May, August, and

Fig. 2 Spatial distribution for monthly precipitation trends during 1971–2015. “+” denotes that trend is significant at the 0.05 significance level



September. Trend rates of the time coefficients in April, May, and September were -1.3 , -1.5 , and -1.2 per decade, signifying significant dryness trends in those months. The trend rate in August was 1.2 per decade, indicating a significant wetness trend in August.

In April, June, July, and August, spatial coefficients of the second EOF mode were <0 in northern Zhejiang and >0 in southern Zhejiang. The coefficient in May was >0 in northern Zhejiang and <0 in southern Zhejiang, i.e., dryness/wetness patterns were anti-phase between those two areas in April–August. In September–October, spatial coefficients of the second EOF mode were >0 in southeastern Zhejiang and <0 in northwestern Zhejiang, so dryness/wetness patterns were anti-phase between those two areas in July–September (Fig. 5). Time coefficients of the second EOF mode showed the variation of these distributions with time. During 1971–2015,

changes of those coefficients were not significant, except in May and September. The trend rate of the time coefficient of the second EOF mode in May was -0.5 per decade, indicating a significant trend of dryness in northern Zhejiang and a trend of wetness in southern Zhejiang. The trend rate in September was 0.8 per decade, revealing a significant trend of wetness in northwestern Zhejiang and a trend of dryness in the southeastern Zhejiang (Fig. 6).

In August and September, spatial coefficients of the third EOF mode were >0 in eastern Zhejiang and <0 in western Zhejiang, so dryness/wetness patterns were anti-phase between the two areas (Fig. 7). For 1971–2015, the trend rate of the time coefficient of the third EOF mode in August was 0.3 per decade, with 0.10 significance level (Fig. 8). This shows a significant trend of dryness in western Zhejiang and a trend of

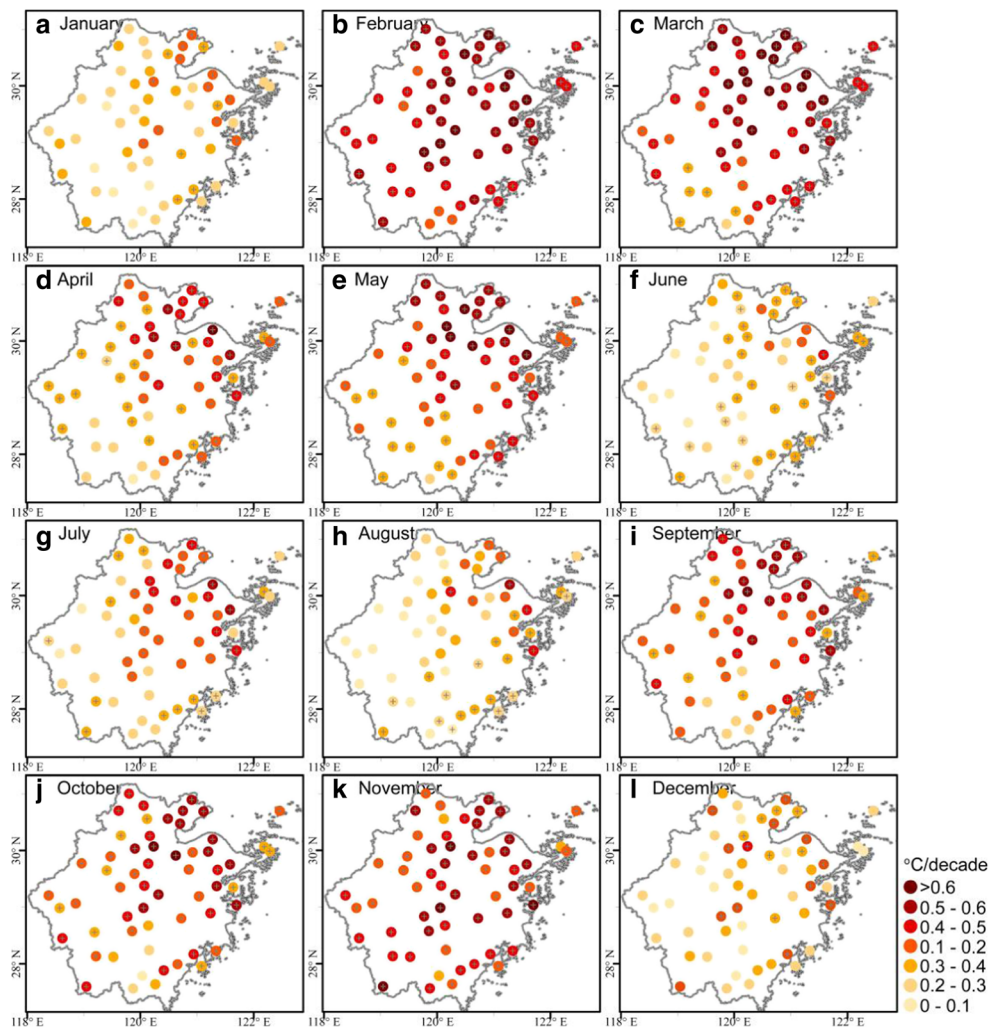


Fig. 3 Spatial distribution for monthly temperature trends during 1971–2015. “+” denotes that trend is significant at the 0.05 significance level

wetness in the eastern Zhejiang. Change of the time coefficient of the third EOF mode in September was not significant.

4 Discussion

The impact factors of spatiotemporal dryness/wetness patterns in Zhejiang may be diverse. In general, the most important

factors associated with such patterns are temperature and precipitation. That is, changes in spatiotemporal features of temperature and precipitation may directly trigger new dryness/wetness patterns in Zhejiang.

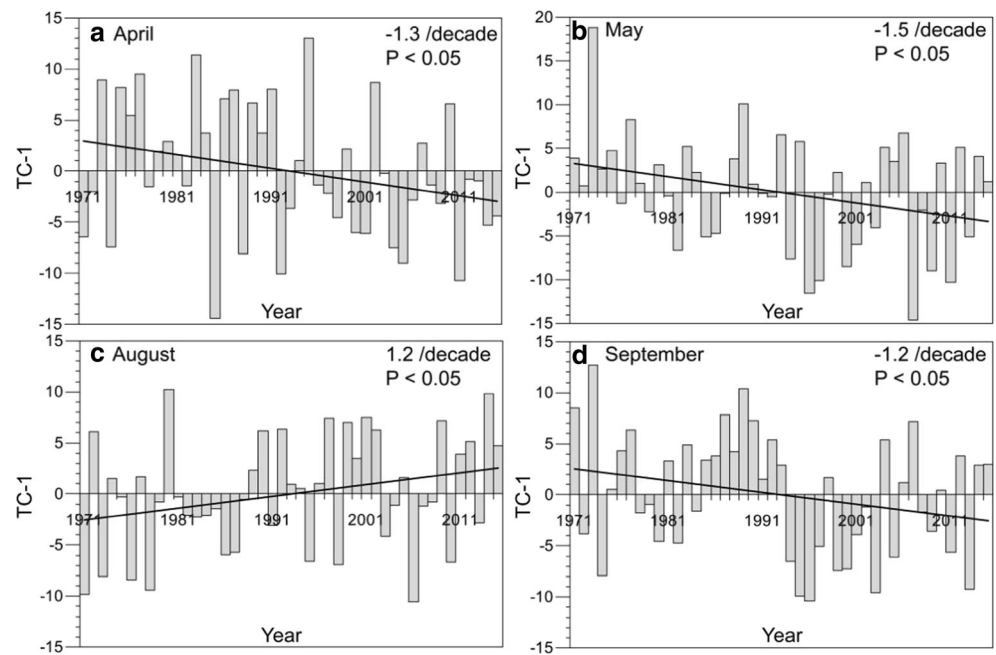
Based on IPCC AR5, annual average precipitation trends have had no statistically significant change, annual average temperature increased significantly at 0.23 °C per decade, and drought events had increasing trends and heavy

Table 1 Contribution of variance of top three modes in EOF analysis based on SPEI for Zhejiang

Mode		Jan	Feb	Mar	Apr	May	Jun	Jul	Aug	Sep	Oct	Nov	Dec
1	CV	78.8	71.5	83.2	69.0	66.0	51.1	62.1	49.8	56.5	69.2	75.9	87.1
	ACV	78.8	71.5	83.2	69.0	66.0	51.1	62.1	49.8	56.5	69.2	75.9	87.1
2	CV	10.3	18.8	8.4	11.1	11.3	22.6	10.3	15.8	9.1	9.8	9.3	6.7
	ACV	89.1	90.3	91.6	80.1	77.1	73.7	72.4	65.6	65.6	79.0	85.2	93.8
3	CV	2.6	3.1	1.8	4.7	3.9	6.4	5.6	6.2	6.5	8.2	4.6	1.7
	ACV	91.7	93.4	93.4	84.8	81.0	80.1	78.0	71.8	72.1	87.2	89.8	95.5

CV contribution of variance, ACV accumulated contribution of variance

Fig. 4 Time coefficient of the first EOF mode of SPEI for Zhejiang



precipitation events intensified since the 1970s in China (Intergovernmental Panel on Climate Change (IPCC) 2014). In Zhejiang, although precipitation in some months had significant increasing or decreasing trends, annual average precipitation showed no significant change since 1970. Annual average temperature increased significantly at $0.34\text{ }^{\circ}\text{C}$ per decade, with 0.01 significance level. Dryness/wetness patterns refer to water deficit or excess. Although such patterns are mainly determined by precipitation, in drought periods, high temperature aggravates water deficits through increased evaporation and affects the drought severity. With a significant temperature increase, drought would be aggravated. During May–September, temperatures were $\geq 18\text{ }^{\circ}\text{C}$ in all counties of Zhejiang, plants grew vigorously, and the effect of temperature increase on the dryness pattern was stronger than on the wetness pattern. Since 1970, average temperature during May–September increased significantly at $0.30\text{ }^{\circ}\text{C}$ per decade. The number of counties and months (NCM) for which SPEI was ≤ -1.5 and > -2.0 increased by 1.86 per decade, with 0.10 significance level. The NCM for which SPEI was ≤ -2.0 increased by 1.83 per decade, with 0.05 significance level. The NCM for which SPEI was > -1.5 had no statistically significant change (Fig. 9). Thus, with the significant temperature increase, drought events and intensity increased greatly, whereas the wetness pattern had no significant change during May–September. For example, in the summers of 2003 and 2013, there were most serious heat waves and drought in Zhejiang since 1950.

Generally, all counties were affected by identical large-scale atmospheric circulations, showing consistent dryness/wetness patterns in each month. During April, May, and September, cold air affected Zhejiang and precipitation had

decreasing trends (Chen 2014), and temperature had an increasing trend. These produced an increasing trend of drought events. During August, with climate warming, tropical cyclone precipitation in Zhejiang has had an increasing trend, and there is a tendency toward a wetness pattern (Liu et al. 2013a, b). In January–March and November–December, dryness/wetness patterns were simple under stable northwest airflow control. In April–October, Zhejiang is affected by both cold and warm airflows, and differences of precipitation and temperature caused the differences in dryness/wetness patterns between northern and southern Zhejiang. In August–September, differences of tropical cyclone precipitation gave rise to the difference of dryness/wetness pattern between eastern and western Zhejiang.

Large-scale atmospheric circulations may be another important contributor, which may have been responsible for the evolution of dryness/wetness conditions in time and space, because those circulations can bring water vapor for precipitation and alter key components (e.g., streamflow, soil moisture, and evaporation) of the hydrologic cycle (Liu et al. 2013a, b). Generally, East Asian summer monsoon weakening leads to a wet summer in Zhejiang (Wang 2001). Interannual variations of the tropical monsoon and precipitation over the South China Sea are negatively correlated with southwesterly winds and precipitation over the Yangtze River middle–lower reaches during June and July. Corresponding to a stronger (weaker) tropical monsoon and precipitation, southwesterly winds are weaker (stronger), leading to a dry (wet) June and July in Zhejiang. In addition, because the El Niño–Southern Oscillation has long been recognized as a major cause of Asian summer monsoon variability (including the East Asian and India monsoon systems), it may also have a

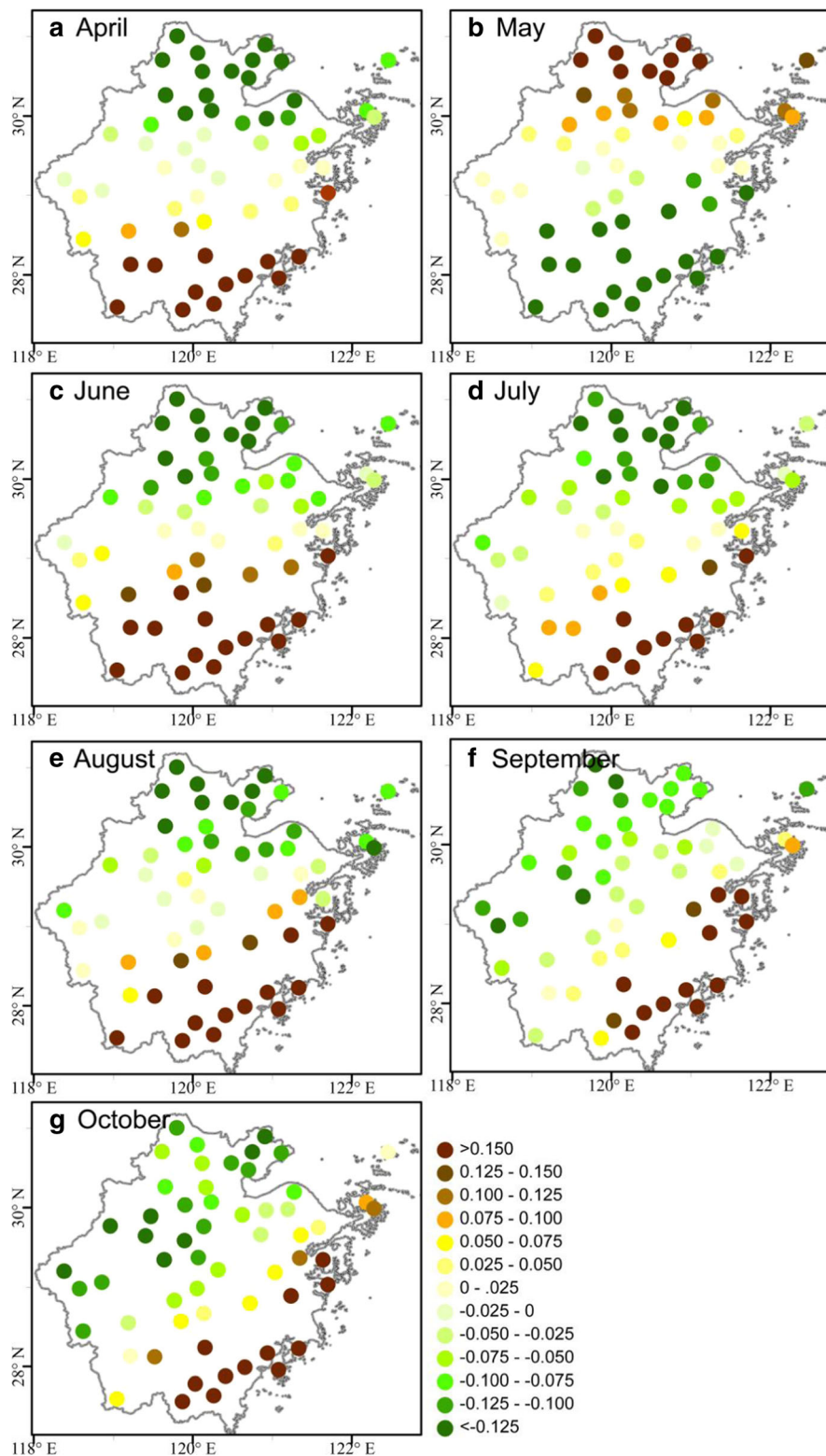


Fig. 5 Spatial distribution of the second EOF mode of SPEI for Zhejiang

teleconnection with the dryness/wetness pattern in Zhejiang. In El Niño events during boreal autumn and winter, rainfall is greater than normal, leading to a wet autumn and winter. During an El Niño event decay phase, there is a wet spring

and dry summer. La Niña events are conducive to invigorating the East Asian winter monsoon and intrusion of cold air southward but are not conducive to the northward transport of warm air from the southwest, leading to a dry winter and spring.

Fig. 6 Time coefficient of the second EOF mode of SPEI for Zhejiang

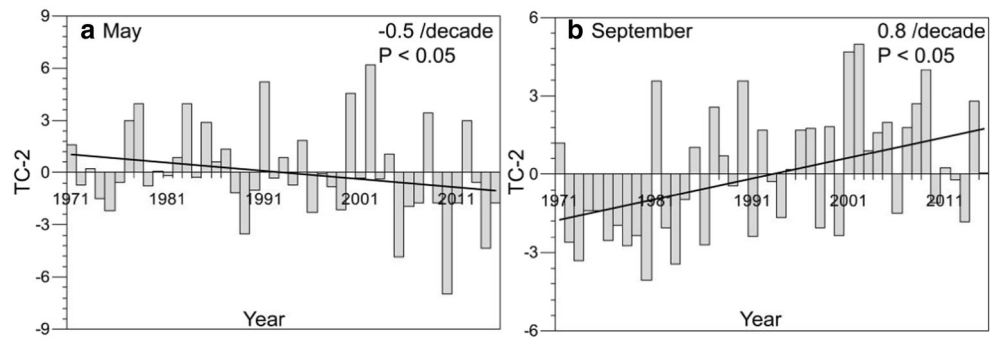
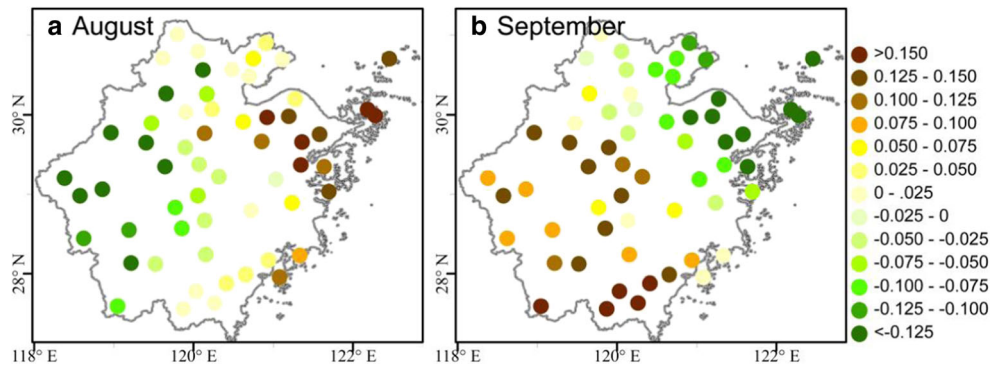


Fig. 7 Spatial distribution of the third EOF mode of SPEI for Zhejiang



5 Conclusions

Climate change has a considerable impact on humans, and it is critical to study regular patterns of meteorological and hydrological factors. The present study explored spatiotemporal characteristics of monthly precipitation, temperature, and SPEI changes during 1971–2015 in Zhejiang Province. The main findings are summarized as follows.

1. Since 1970, similar to China’s regional precipitation in IPCC AR5, annual average precipitation had no

significant change. Precipitation in April, May, September, and October had decreasing trends and increasing trends in November and December. Changes of precipitation in other months were not significant. Monthly precipitation was the main control on the SPEI, and trends of precipitation and SPEI were found to be identical.

2. Monthly temperatures had significant increasing trends in Zhejiang. Since 1970, the annual average temperature rate of increase has been larger than China’s regional temperature by 0.11 °C per decade. During May–September, the effect of temperature increase on the dryness pattern was stronger than on the wetness pattern. With significant temperature increase, drought events and intensity increased significantly, while the wetness pattern showed no significant change.

3. There were three distributions of dryness/wetness patterns in Zhejiang Province. The first EOF mode showed consistent dryness/wetness patterns in Zhejiang. There were significant dryness trends in April, May, and September, a wetness trend in August, and no dryness/wetness pattern changes in other months. The second EOF mode revealed anti-phase dryness/wetness patterns between northern and southern Zhejiang during April–October. Because of cold and warm airflow changes, there was a dryness trend in

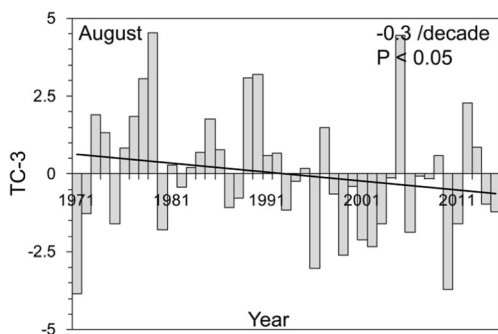
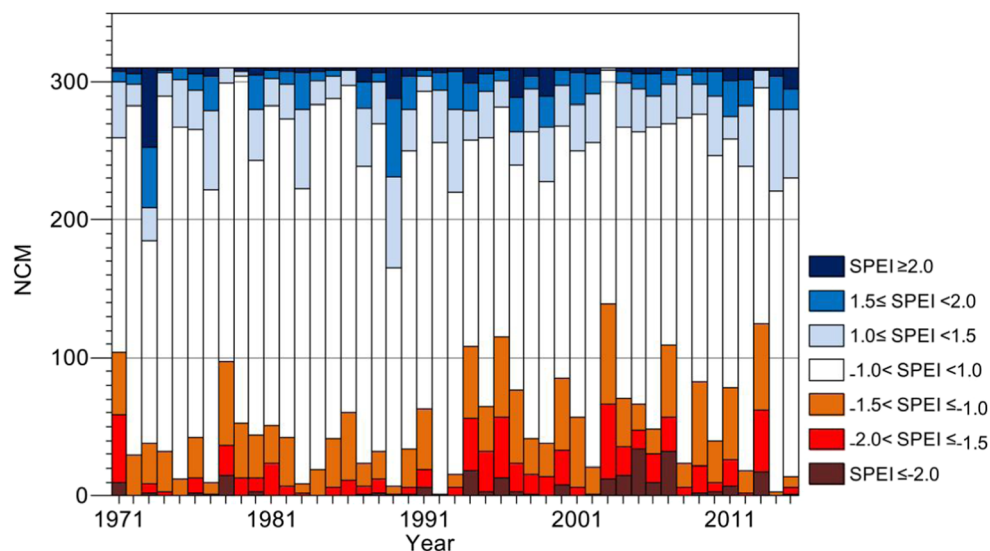


Fig. 8 Time coefficient of the third EOF mode of SPEI for Zhejiang

Fig. 9 Change of number of counties and months (NCM) in different SPEI levels in Zhejiang during 1971–2015



northern Zhejiang and a wetness trend in southern Zhejiang during May, as well as a wetness trend in north-western Zhejiang and dryness trend in southeastern Zhejiang during September. Because of differences in tropical cyclone precipitation, there was a third difference in dryness/wetness pattern between eastern and western Zhejiang during August–September, and there was a wetness trend in eastern Zhejiang and dryness trend in western Zhejiang during August.

Acknowledgements This paper was financially supported by a major agricultural grant from the Science Technology Department of Zhejiang Province, China (No. 2011C22082), and by the Disaster Research Fund of the People's Insurance Company of China (Study and Application on Weather Index Insurance).

References

- Allen RG, Pereira LS, Raes D, Smith M (1998) Crop evapotranspiration. Guidelines for computing crop water requirements. *Fao Irrigation and Drainage Paper*, 56
- Chen S (2014) A study of the climatic anomaly of the spring precipitation in southern China. *Clim Chang Res Lett* 03(1):6–12
- Dubrovsky M, Svoboda MD, Trnka MJ et al (2009) Application of relative drought indices in assessing climate-change impacts on drought conditions in Czechia. *Theor Appl Clim* 96(1–2):155–171
- Ercha A, Zhang D, Ridley AJ, Xiao Z, Hao Y (2012) A global model: empirical orthogonal function analysis of total electron content 1999–2009 data. *J Geophys Res Atmos* 117(A3):1–83
- Feng S, Hu Q, Qian W (2004) Quality control of daily meteorological data in China 1951–2000: a new dataset. *Int J Climatol* 24:853–870
- Fischer T, Gemmer M, Lüliu L et al (2011) Temperature and precipitation trends and dryness/wetness pattern in the Zhujiang River Basin, South China, 1961–2007. *Quat Int* 244(2):138–148
- Gocic M, Trajkovic S (2014) Drought characterisation based on water surplus variability index. *Water Resour Manag* 28(10):3179–3191
- Guo L, Xia Z (2014) Temperature and precipitation long-term trends and variations in the Ili-Balkhash Basin. *Theor Appl Clim* 115(1–2): 219–229
- Huang J, Sun S, Xue Y et al (2014a) Spatial and temporal variability of precipitation indices during 1961–2010 in Hunan Province, Central South China. *Theor Appl Clim* 118(3):581–595
- Huang J, Sun S, Xue Y et al (2014b) Spatial and temporal variability of precipitation and dryness/wetness during 1961–2008 in Sichuan Province, West China. *Water Resour Manag* 28(6):1655–1670
- Intergovernmental Panel on Climate Change (IPCC) (2014) ‘Detection and Attribution of Climate Change: from Global to Regional’ Chapter 10 in *Climate Change 2013: The Physical Science Basis*. Available at: <https://www.ipcc.ch/report/ar5/wg1/>
- Kaihatu JM, Handler RA, Marmorino GO, Shay LK (1998) Empirical orthogonal function analysis of ocean surface currents using complex and real-vector methods. *J Atmos Ocean Technol* 15:927–941
- Liu Z, Zhou P, Zhang F et al (2013a) Spatiotemporal characteristics of dryness/wetness conditions across Qinghai Province, Northwest China. *Agric For Meteorol* 182–183:101–108
- Liu T, Wu L, Zhang J, Ren F (2013b) Analysis of tropical cyclone precipitation changes in China in July–September during 1965–2010. *Acta Meteorological Sinica* 71(1):63–75
- Livada I, Assimakopoulos VD (2007) Spatial and temporal analysis of drought in Greece using the standardized precipitation index (SPI). *Theor Appl Climatol* 89:143–153
- Lorenzo-Lacruz J, Vicente-Serrano SM, López-Moreno JI et al (2010) The impact of droughts and water management on various hydrological systems in the headwaters of the Tagus River (Central Spain). *J Hydrol* 386(1–4):13–26
- McKee TB, Doesken NJ, Kleist J (1993) The relationship of drought frequency and duration to time scales. Preprints, Eighth Conf. on Applied Climatology. Anaheim, CA, Amer. Meteor. Soc. 179–184
- Patel NR, Chopra P, Dadhwal VK (2007) Analyzing spatial patterns of meteorological drought using standardized precipitation index. *Meteorol Appl* 14(4):329–336
- Potop V, Možný M, Soukup J (2012) Drought evolution at various time scales in the lowland regions and their impact on vegetable crops in the Czech Republic. *Agric For Meteorol* 156(8):121–133
- Potop V, Boroneanț C, Možný M, Štěpánek P, Skalák P (2014) Observed spatiotemporal characteristics of drought on various time scales over the Czech Republic. *Theor Appl Clim* 115(3–4):563–581
- Qian W, Lin X (2004) Regional trends in recent temperature indices in China. *Clim Res* 27:119–134

- Qian W, Lin X (2005) Regional trends in recent precipitation indices in China. *Meteorog Atmos Phys* 90(3–4):193–207
- Rebetez M, Mayer H, Dupont O et al (2006) Heat and drought 2003 in Europe: a climate synthesis. *Ann For Sci* 63:569–577
- Sen PK (1968) Estimates of regression coefficient based on Kendall's tau. *J Am Stat Assoc* 63:1379–1389
- Shen J, Hu B (2005) Analysis of laws and sudden-change of drought/flood for last 534 years in Zhejiang Province. *Meteorological Monthly* 31(10):76–79 (in Chinese)
- Stagge JH, Tallaksen LM, Gudmundsson L et al (2015) Candidate distributions for climatological drought indices (SPI and SPEI). *Int J Climatol*. doi:10.1002/joc.4267
- Vicente-Serrano SM, Beguería S, López-Moreno JI (2010) A multiscalar drought index sensitive to global warming: the standardized precipitation evapotranspiration index. *J Clim* 23(7):1696–1718
- Vicente-Serrano SM, Beguería S, López-Moreno JI et al (2012) Performance of drought indices for ecological, agricultural, and hydrological applications. *Earth Interact* 16(3):1–27
- Wang H (2001) The weakening of the Asian monsoon circulation after the end of 1970's. *Adv Atmos Sci* 18(3):376–386
- Yusof F, Hui-Mean F, Suhaila J et al (2014) Rainfall characterisation by application of standardised precipitation index (SPI) in peninsular Malaysia. *Theor Appl Clim* 115(3–4):503–516
- Zhai J, Su B, Krysanova V et al (2010) Spatial variation and trends in PDSI and SPI indices and their relation to streamflow in 10 large regions of China. *J Clim* 23(3):649–663
- Zhang Q, Xu CY, Zhang Z (2009) Observed changes of drought/wetness episodes in the Pearl River Basin, China, using the standardized precipitation index and aridity index. *Theor Appl Clim* 98(1–2): 89–99